Rate Coefficients of Hydroxyl Radical Reaction with Dimethyl Ether and Methyl *tert*-Butyl Ether over an Extended Temperature Range

Muhammad Arif,† Barry Dellinger, and Philip H. Taylor*

Environmental Sciences and Engineering, University of Dayton Research Institute, 300 College Park, Dayton, Ohio 45469-0132

Received: October 9, 1996; In Final Form: January 24, 1997[⊗]

Rate coefficients of the reaction of hydroxyl (OH) radicals with CH_3OCH_3 (k_1) and $CH_3OC(CH_3)_3$ (k_2) over an extended temperature range are reported. Measurements were performed using a laser photolysis−laser-induced fluorescence technique under slow flow conditions at a total pressure of 740 ± 10 Torr. Arrhenius plots of the data exhibited significant curvature and were fitted in the form of $k(T) = AT^B \exp(-C/T)$. The resulting modified Arrhenius expressions (error limits $\pm 2\sigma$) that best described these extended temperature measurements and prior low-temperature measurements were (in units of cm^3 $molecule^{-1}$ s^{-1}) $k_1(295-650\ K) = (1.05 \pm 0.10) \times 10^{-17} T^{2.0} \exp[(328 \pm 32)/T]$ and $k_2(293-750\ K) = (1.15 \pm 0.11) \times 10^{-17} T^{2.04} \exp[(266 \pm 41)/T]$. Comparison of our measurements for k_1 with previous, overlapping low-temperature measurements indicated generally good agreement. Our measurements for k_2, although consistent with previous room temperature measurements, exhibited a larger temperature dependence than previously reported. High-temperature oxidation mechanisms for these oxygenated fuel components are proposed. Support for the mechanisms is presented in the form of product analysis studies in high-temperature tubular flow reactors. For $CH_3OC(CH_3)_3$, these studies suggest that H abstraction from the *tert*-butyl group is an important high-temperature oxidation pathway.

Introduction

Reaction with hydroxyl (OH) radicals is an important step in the oxidation of organic compounds in the atmosphere[1] and in combustion systems.[2] Ethers represent important classes of organic compounds due to their wide use as solvents in industry, e.g., industrial painting facilities, the manufacturing of perfumes and flavorings, pharmaceutical plants, textile manufacturers, can coating plants, airplane manufacturers, electronic component plants, etc., as well as their formation as intermediates in hydrocarbon combustion. Thus, accurate kinetic data for the rates of reaction of these species with OH are required to model their chemistry in the atmosphere from industrial releases and in combustion processes.

An important application of oxygenated hydrocarbons is as an additive to reformulated gasoline.[3] Direct emission of the additive and oxygenated combustion byproducts can result in a significant impact on urban and regional ozone problems.[4] Consequently, there has been continued developmental work on improved reformulated gasolines and alternative fuels.[5−11] This research has been aimed at significantly reducing the reactivity (in terms of atmospheric ozone-forming potential) of tail pipe and evaporative emissions, compared to those from conventional gasoline-fueled vehicles, without loss of drivability. However, to understand their atmospheric impact, the mechanism of their atmospheric oxidation must be understood. Furthermore, since these oxygenated hydrocarbons are being used as fuel additives, their reactions and mechanism of oxidation under combustion conditions are also of considerable importance.

In this paper, we present new rate coefficient measurements for the reactions of OH radicals with dimethyl ether (CH_3OCH_3) and methyl *tert*-butyl ether ($CH_3OC(CH_3)_3$). The measurements were obtained over a much wider temperature range than previously investigated. Mechanistic pathways for the high-temperature oxidation of these compounds are proposed. Support for these pathways is provided by product analyses from high-temperature, fused silica flow reactor experiments. The mechanistic pathways are compared with previous atmospheric temperature, smog chamber experiments.[12,13]

Experimental Approach and Data Reduction

The experimental procedures were similar to previous studies of OH reactions with chlorinated hydrocarbons[14,15] and hydrochlorofluorocarbons.[16] Hence, we only briefly summarize them here.

OH radicals were produced by 193.3 nm photodissociation of reactant/N_2O/H_2O/He gas mixtures with an ArF excimer laser (Questek Model 2860). Initial OH concentrations, $[OH]_0$, ranged from 2×10^{10} to 1×10^{11} molecules cm^{-3} and were determined from measured photolysis laser fluences, published values of the N_2O absorption coefficient (8.95×10^{-20} cm^2 $molecule^{-1}$ at 298 K),[17] a photodissociation quantum yield for $O(^1D)$ production of unity,[18] and assumption of the rapid reaction of $O(^1D)$ with H_2O (95% conversion in $<20\ \mu s$). Experiments were conducted for photolysis laser intensities of 1−5 mJ cm^{-2}. Following reaction initiation, time-resolved OH profiles were measured as functions of reactant concentration using laser-induced fluorescence with a pulsed Nd:YAG pumped-dye laser (Quanta Ray Model DCR-2/PDL-2) emitting at the wavelength of 282.1 nm. Broad-band fluorescence was collected at 309 nm using a PMT/band-pass filter combination.

In order to control the temperature uniformly, four symmetrical ceramic heaters surrounded the optical reactor adjacent to the reaction zone. The gas temperature was measured with a chromel−alumel thermocouple positioned ~3 mm from the probe intersection volume. Measurements using a second retractable chromel−alumel thermocouple indicated a maximum variation of less than 4 K across the probe volume for gas

† Ph.D. Candidate in Electro-Optics.
* To whom correspondence should be addressed.
[⊗] Abstract published in *Advance ACS Abstracts,* March 1, 1997.

S1089-5639(96)03119-2 CCC: $14.00

TABLE 1: Absolute Rate Coefficients for k_1 (in cm^3 molecule^{-1} s^{-1})

temp, K	$10^{12}k_1$	$10^{12}\sigma_{k_1}$	temp, K	$10^{12}k_1$	$10^{12}\sigma_{k_1}$
295	2.95	0.21	490	4.62	0.25
346	3.42	0.18	549	6.27	0.31
396	3.73	0.20	601	7.12	0.47
455	4.20	0.11	650	8.19	0.39

temperatures ranging from 295 to 1000 K.[19] All experiments were performed under slow flow conditions, and the buildup of reaction products was minimized. Individually controlled gas flows of reactant/N_2O/H_2O/He were thoroughly mixed before entering the optical reactor. The composite flow conditioned the reactor for 1−3 min prior to the onset of data collection, thereby minimizing any effects due to reactant adsorption on the reactor walls. Experiments were conducted at a helium pressure of 740 ± 10 Torr.

All experiments were performed with the reactant in great excess of OH, i.e., $[\text{reactant}]_0 > 500[\text{OH}]_0$. Hence, exponential OH radical decays resulting in measurement of a pseudo-first-order decay constant $k' = k_{bi}[\text{reactant}] + k_d$ were expected. In this expression, k_{bi} is the true bimolecular rate coefficient for the reaction of OH with the reactant, and k_d represents OH decay due to diffusion and reaction with impurities in the probe volume. For all experiments, OH radical decay profiles indeed exhibited exponential behavior and were fitted by the following nonlinear expression

$$[\text{OH}] = [\text{OH}]_0 \exp(-k't) + \gamma$$

where γ is the constant background signal level and t is the time delay between the two lasers. The bimolecular rate constant, k_{bi}, was obtained from a least-squares analysis of k' versus the initial reactant concentration. Excellent statistical correlations ($r^2 > 0.995$) were obtained from the analysis of bimolecular rate coefficients for both k_1 and k_2.

Samples of CH_3OCH_3 and $CH_3OC(CH_3)_3$ were obtained from Aldrich, Inc. Gas chromatography−mass spectrometry (GC-MS) analyses indicated that CH_3OCH_3 was free of contaminants (>99.9% pure). GC-MS analysis of $CH_3OC(CH_3)_3$ indicated very small (<0.1%) amounts of methyl formate and methanol as impurities. These impurities reacted with OH at a much slower rate than $CH_3OC(CH_3)_3$ and did not affect the rate measurements. The remaining chemicals used in our gas delivery system had the following stated minimum purities: He (99.999+%), N_2O (99.9%), H_2O (HPLC organic-free reagent grade). Absorption cross sections for the reactants were very small (on the order of 10^{-21} cm^2 molecule^{-1})[20] compared with N_2O at 193 nm. Thus, laser photolysis of the reactants was expected to be insignificant. This was verified by numerous experiments where variation of the excimer laser intensity from 1 to 5 mJ/cm^2 had no observable effect on OH decays. The possibility that OH decays could be due to reaction with photolytically generated but unreacted O atoms was investigated by varying the H_2O concentration. Bimolecular rate determinations were unaffected by factor of 5 changes in H_2O, indicating that unreacted O atoms had no effect on the observed measurements.

Experimental Results and Discussion

CH_3OCH_3 + OH. Measurements for the reaction of OH + CH_3OCH_3 (k_1) between temperatures of 295 and 650 K are summarized in Table 1. Also shown in Table 1 are standard deviations in the rate measurements indicating 2σ uncertainties ranging from ±5 to ±14%.

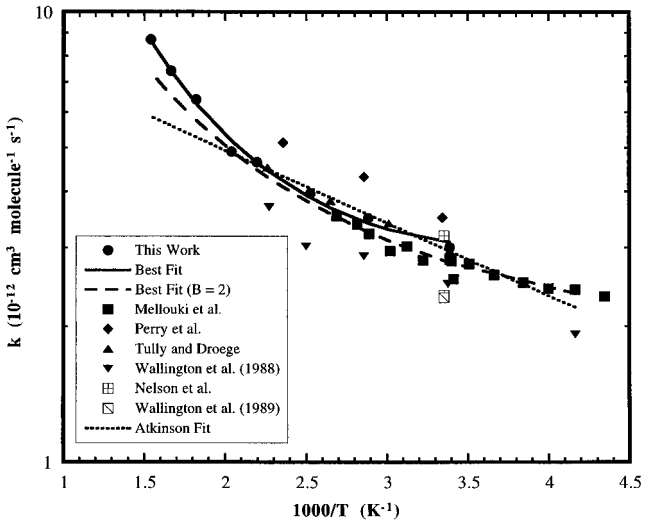

Figure 1. Arrhenius plot of experimental rate measurements for k_1. Also shown are previous experimental studies,[21−26] Atkinson's,[27] recommendation, and our best fit experimental recommendation.

Measurements at temperatures of 700 and 750 K resulted in lower rate constants ((∼7−8) × 10^{-12} cm^3 molecule^{-1} s^{-1}). This deviation was attributed to reactant thermal decomposition. To our knowledge, this is the first report of experimental measurements for this reaction above temperatures of 440 K.

There have been six prior studies of the gas-phase reaction of k_1.[21−26] Five of these have been conducted as a function of temperature, with the experiments of Tully and Droege[22] considered the most accurate. The results are summarized in Arrhenius form in Figure 1.

The available temperature-dependent data were best described by a simple Arrhenius expression. This reaction is believed to proceed by H-atom abstraction from the CH_3 groups. The lack of any π bonds in the substrate rules against the possibility of OH addition. The lack of a pressure effect was verified by Wallington et al.[23,24] The rate coefficient per C−H bond for CH_3OCH_3 is similar to the reaction of OH radicals with secondary C−H bonds in alkanes.[21] This is to be expected, since the C−H bond strength in CH_3OCH_3 is 93 ± 1 kcal/mol, similar to the secondary C−H bond strength in *n*-butane of 95 ± 1 kcal/mol. Tully and Droege[22] attempted to acquire data above 440 K, but unidentified secondary processes interfered with the kinetics.

We have obtained measurements for k_1 between temperatures of 295 and 650 K. A comparison of these measurements with previous measurements is shown in Figure 1. The rate constant measurements between 295 and 440 K are in excellent agreement with the previous measurements of Tully and Droege[22] and the recommended Arrhenius expression given by Atkinson.[27] The rate constant measurements of Perry et al.[21] and Wallington et al.[23,24] are displaced approximately equally above and below the more recent LP/LIF measurements. Above 500 K, significant curvature in the Arrhenius plot was observed. A nonlinear least-squares analysis of our measurements ($\chi^2 = 4.89$, see Figure 1) is given by the following modified Arrhenius expression (error limits ±1σ) in units of cm^3 molecule^{-1} s^{-1}:

$$k_1(295-650\text{ K}) = (3.39 \pm 13.8) \times 10^{-24} T^{(4.11\pm0.6)} \times \exp[(1221 \pm 252)/T]$$

The empirical "best fit" expression results in an unreasonably large value for the curvature in the Arrhenius plot ($B = 4.11$). Furthermore, below 295 K, considerable disparity exists between extrapolated rate coefficients based on our empirical "best fit"

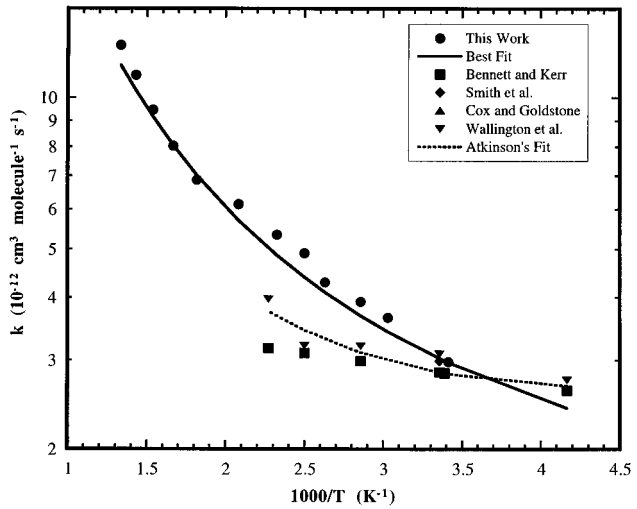

Figure 2. Arrhenius plot of experimental rate measurements for k_2. Also shown are previous experimental studies,[24,28−30] Atkinson's[27] recommendation, and our best fit experimental recommendation.

TABLE 2: Absolute Rate Coefficients for k_2 (in cm^3 molecule^{-1} s^{-1})

temp, K	$10^{12}k_2$	$10^{12}\sigma_{k_2}$	temp, K	$10^{12}k_2$	$10^{12}\sigma_{k_2}$
293	2.98	0.11	480	6.15	0.52
330	3.65	0.22	550	6.86	0.30
350	3.92	0.30	600	8.03	0.25
380	4.30	0.49	650	9.45	0.47
400	4.91	0.23	700	11.1	0.90
430	5.34	0.37	750	12.7	0.51

expression and the previous measurements by Wallington et al.[23] and Mellouki et al.[26] The modified Arrhenius expression based loosely on transition state theory, i.e., the temperature exponent B fixed at a value of 2.0, results in a reasonable fit to the combined low-temperature (230−295 K) measurements of Mellouki et al.[26] and the new higher temperature data generated in this study (cf. Figure 1). This fit ($\chi^2 = 17.50$, error limits $\pm 1\sigma$) in units of cm^3 molecule^{-1} s^{-1} is given by

$$k_1(295-650\ \mathrm{K}) = (1.05 \pm 0.05) \times 10^{-17} T^{2.0} \times \exp[(328 \pm 16)/T]$$

and is recommended for both atmospheric chemistry and combustion modeling purposes.

$CH_3OC(CH_3)_3$ + OH. Measurements for the reaction of OH + $CH_3OC(CH_3)_3$ (k_2) between temperatures of 293 and 750 K are summarized in Table 2. Also shown in Table 2 are standard deviations in the rate measurements indicating 2σ uncertainties ranging from ±7 to ±23%.

Measurements above 750 K did not produce a linear relationship between pseudo-first-order rate constant, k', and reactant concentration and were interpreted to indicate reactant thermal decomposition.

There have been four prior measurements of k_2. They are summarized in Figure 2.[24,28−30]

The room temperature data from these four studies are in fairly good agreement. The data of Wallington et al.[24] and Bennett and Kerr[29] represent the only temperature-dependent studies, albeit over a narrow range. The data are equally well represented by a simple Arrhenius or a modified Arrhenius expression.[27] The reaction is believed to proceed by H atom abstraction. The lack of any π bonds in the substrate rules against the possibility of OH addition. Product analysis in smog chamber experiments at room temperature verified the H abstraction mechanism and also indicated that H atom abstraction from the methoxy group and the *tert*-butyl group accounted for ∼70−85% and ∼20% of the overall reaction, respectively.[14,15] The greater reactivity of the methoxy group is consistent with the results for dimethyl ether, where the C−H bond strength is reduced by direct bonding of the primary carbon to oxygen.

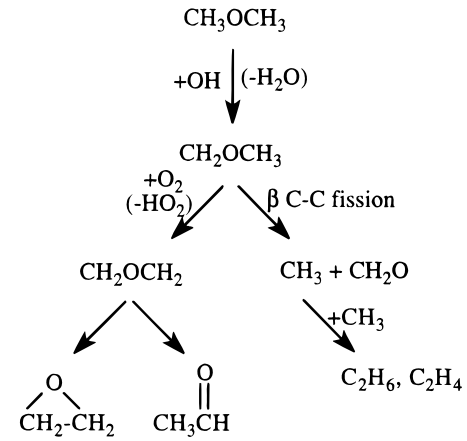

Figure 3. Reaction pathway diagram for CH_3OCH_3 oxidation. Pathways for oxidation of CH_2O are removed for clarity.

Our measurements at room temperature were in good agreement with previous measurements. However, at higher temperatures, we observed a larger temperature dependence than previously reported and significant curvature in the Arrhenius plot. In light of the care taken to avoid reactant photolysis and errors in reactant concentration due to surface adsorption, reasons for the discrepancy between our data and previous measurements are unclear at this time. A nonlinear least-squares analysis of our data ($\chi^2 = 9.74$) resulted in the following modified Arrhenius expression (error limits $\pm 1\sigma$) in units of cm^3 molecule^{-1} s^{-1} (denoted as best fit in Figure 2):

$$k_2(293-750\ \mathrm{K}) = (1.11 \pm 3.18) \times 10^{-17} T^{(2.04\pm0.4)} \times \exp[(266 \pm 177)/T]$$

Mechanistic Pathways. Numerous experimental and modeling studies[31] have shown that reactions of the hydroxyl radical are important in the high-temperature oxidation of organic compounds. Thermal instrumentation systems consisting of fused silica helical flow reactors coupled with in-line gas chromatographic−mass spectrometric analysis have been recently used to study the high-temperature oxidation of alternative fuels in this laboratory.[5,9−11] These atmospheric pressure experiments have examined the gas-phase, near-stoichiometric, oxidative conversion of methanol, ethanol, M85, E85, natural gas, LP gas, and reformulated gasoline at temperatures of 773−1273 K for reaction times of 0.9−2.0 s. In typical experiments, vapor-phase, near-stoichiometric mixtures of fuel and oxygen are premixed *a priori* in 2 L glass vessels and injected into the flow reactor using high-purity helium as the diluent and carrier gas at initial concentrations ranging from 300 to 1000 ppmv.

To shed some insight into the mechanistic details of the hydroxyl radical reactions investigated using the LP/LIF technique (*vide supra*), some additional experiments have examined the near-stoichiometric, oxidative conversion of CH_3OCH_3 and $CH_3OC(CH_3)_3$ using these thermal instrumentation systems. At near-stoichiometric reaction conditions and intermediate temperatures, reactions of hydroxyl radicals are expected to become increasingly important with respect to initial reactant conversion compared to hydroperoxy radicals, which dominate conversion of oxygenated fuels at lower temperatures.[2]

Figure 3 presents a reaction pathway diagram for CH_3OCH_3 oxidation. H abstraction results in the formation of CH_3OCH_2

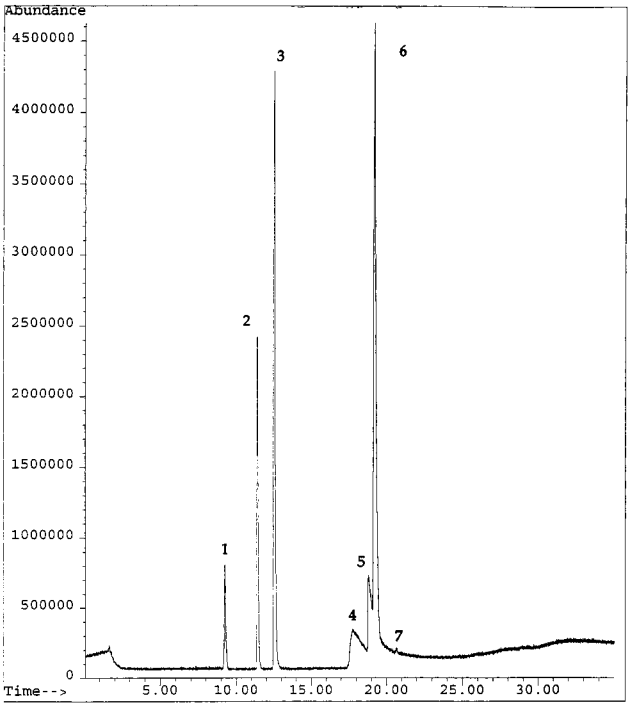

Figure 4. Total ion chromatogram of the stoichiometric oxidation of CH_3OCH_3. Reactor temperature = 1053 K, residence time = 0.85 s, initial gas-phase CH_3OCH_3 concentration = 500 ppm. Legend: 1, carbon dioxide; 2, ethene; 3, ethane; 4, formaldehyde; 5, water; 6, dimethyl ether; 7, acetaldehyde or ethylene oxide.

radicals. The fate of CH_3OCH_2 is not well understood. Previous low-temperature smog chamber studies[12] indicated that the major reaction product under simulated atmospheric conditions was methyl formate, $HCOOCH_3$. Following H abstraction by OH radicals, this product formed as a result of a series of reactions involving O_2 addition, O atom abstraction by NO, H abstraction by O_2, followed by isomerization to yield $HCOOCH_3$. At elevated temperatures, the primary route of O_2 attack will be H abstraction. This will result in the formation of the $^{\bullet}CH_2-O-{}^{\bullet}CH_2$ diradical. The potential fate of this diradical includes isomerization to ethylene oxide or acetaldehyde. An alternative fate for CH_3OCH_2 is β C−O bond cleavage resulting in the formation of $CH_3 + CH_2O$.

A total ion chromatogram from the stoichiometric oxidation of CH_3OCH_3 (T = 1053 K) is illustrated in Figure 4. The major reaction products are ethane, formaldehyde, and ethene. A minor reaction product is ethylene oxide or acetaldehyde. (The signal-to-noise ratio of the ethylene oxide or acetaldehyde peak did not allow clear mass spectral discrimination of these two species.) Methyl formate was not observed among the reaction products. The distribution of products suggests that the primary fate of the CH_3OCH_2 radical is β C−O bond cleavage. Additional flow reactor experiments were carried out at slightly lower temperatures (923, 1003, and 1013 K) and higher temperatures (1073 K) to determine whether ethane, formaldehyde, and ethene may have formed as secondary reaction products from the decomposition of ethylene oxide or acetaldehyde. Neither ethylene oxide (or acetaldehyde) nor any of their secondary oxidation products were observed to be major reaction products under any of these conditions.

Figure 5 presents a reaction pathway diagram for $CH_3OC(CH_3)_3$ oxidation. OH radicals can abstract H atoms from either the methoxy group or the *tert*-butyl group. Previous low-

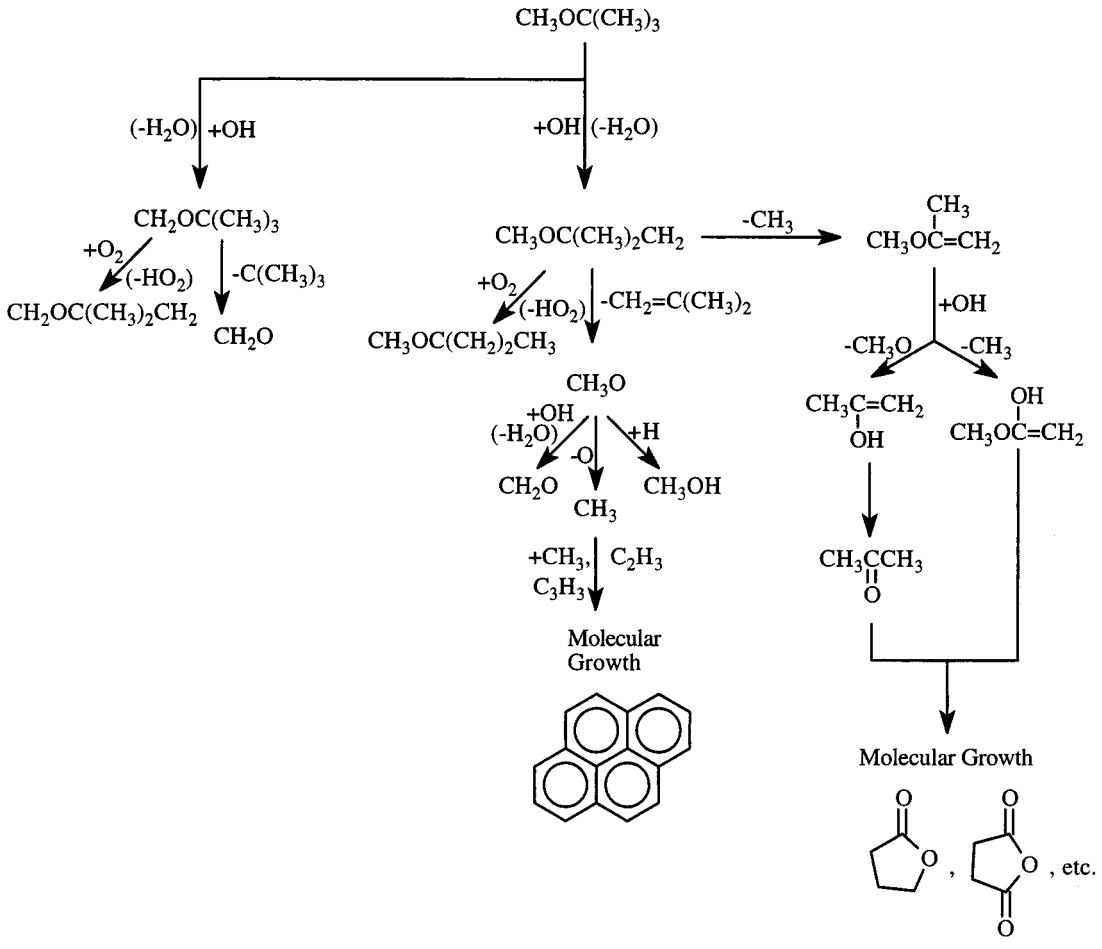

Figure 5. Reaction pathway diagram for $CH_3OC(CH_3)_3$ oxidation. Pathways for oxidation of CH_2O are removed for clarity.

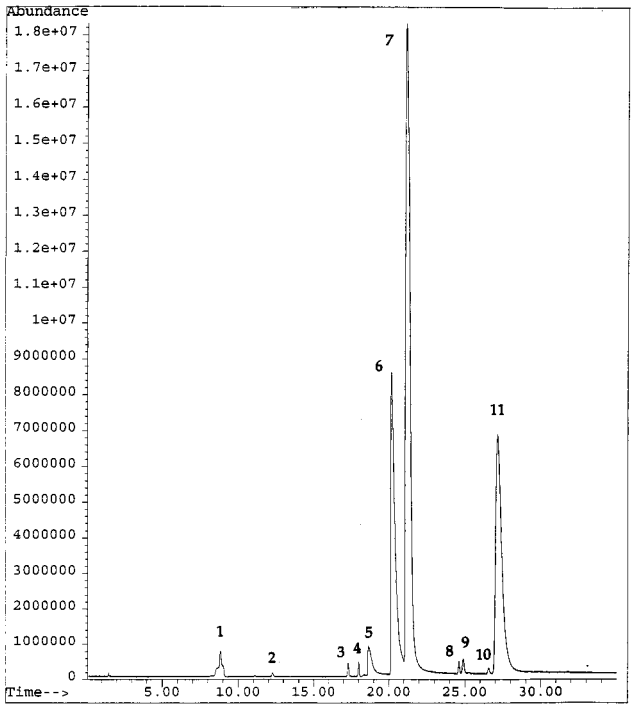

Figure 6. Total ion chromatogram of the stoichiometric oxidation of $CH_3OC(CH_3)_3$. Reactor temperature = 918 K, residence time = 0.85 s, initial gas-phase $CH_3OC(CH_3)_3$ concentration = 500 ppm. Legend: 1, carbon dioxide; 2, ethane; 3, propene; 4, 1,2- propadiene; 5, water; 6, methanol; 7, isobutene; 8, acetone; 9, 1,1-dimethylcyclopropane; 10, C_4 oxygenate; 11, methyl *tert*-butyl ether.

temperature smog chamber studies indicated that H abstraction from the methoxy site was dominant.[12,13] The major reaction products under these simulated atmospheric conditions were *tert*-butyl formate, formaldehyde, and methyl acetate. At higher temperatures where the differences in bond strength become less important, one must also consider the entropy favored H abstraction from the *tert*-butyl site, thus resulting in the formation of both $CH_2OC(CH_3)_3$ and $CH_3OC(CH_3)_2CH_2$ radicals. The fate of these oxygenated radicals is not well understood. H abstraction via reaction with molecular oxygen results in the formation of two diradicals, $CH_2OC(CH_2)(CH_3)_2$ and $CH_3OC(CH_2)_2CH_3$. The only conceivable stabilization routes for these diradicals are formation of substituted three- or four-member ring compounds. An alternative fate for $CH_2OC(CH_3)_3$ and $CH_3OC(CH_3)_2CH_2$ radicals is β C−O or C−H bond cleavage. For $CH_2OC(CH_3)_3$, this results in formation of formaldehyde and *tert*-butyl radicals. For $CH_3OC(CH_3)_2CH_2$, the corresponding products are isobutene and methoxy radicals (C−O cleavage) or methylpropenyl ether and methyl radicals (C−H cleavage).

A total ion chromatogram from the stoichiometric oxidation of $CH_3OC(CH_3)_3$ (T = 918 K) is illustrated in Figure 6. The major reaction products were isobutene and methanol. Minor reaction products included ethane, propene, 1,2-propadiene, acetone, 1,1-dimethylcyclopropane, and a C_4 oxygenate. The major atmospheric products, *tert*-butyl formate, formaldehyde, and methyl acetate, were not detected in these high-temperature experiments. The distribution of products suggests that OH attack on the *tert*-butyl group is the dominant initial reaction channel. Furthermore, it appears that the primary mode of decomposition of $CH_3OC(CH_3)_2CH_2$ is β C−O bond cleavage yielding isobutene and methoxy radicals. The lack of detection of three- or four-member ring compounds suggests that molecular oxygen may not play a dominant role in reactions of the initially formed radicals, although this must be substantiated with additional work. The observation of propene and propadiene is conceivable with the subsequent decomposition of isobutene. The formation of acetone and other oxygenated species indicates that other reactions, perhaps initiated by loss of CH_3 from $CH_3OC(CH_3)_2CH_2$, are significant. These routes may result in formation of large ring species incorporating oxygen in their structures. Products of this type have recently been identified using multidimensional gas chromatography−mass spectrometry of the reactor effluent from the oxidation of reformulated gasoline in our laboratories.[31]

Conclusions

New atmospheric pressure, absolute rate measurements are reported for the reaction of hydroxyl radicals with dimethyl ether (k_1) and methyl *tert*-butyl ether (k_2). Arrhenius plots of the data indicated significant curvature. The following modified Arrhenius expressions (in units of cm^3 $molecule^{-1}$ s^{-1}) are thus recommended for use by both atmospheric chemistry and combustion modelers:

$$k_1(295-650\ \mathrm{K}) = 1.05 \times 10^{-17} T^{2.0} \exp[328/T]$$

$$k_2(293-750\ \mathrm{K}) = 1.11 \times 10^{-17} T^{2.04} \exp[266/T]$$

Atmospheric pressure product analysis studies suggest that the dominant fate of the CH_3OCH_2 radical produced in k_1 is β C−O bond cleavage yielding formaldehyde and methyl radicals as the major products. For $CH_3OC(CH_3)_3$, product analyses suggest that OH attack on the *tert*-butyl group is the dominant initial reaction channel at elevated temperatures. Furthermore, it appears that the primary mode of decomposition of $CH_3OC(CH_3)_2CH_2$ is β C−O bond cleavage yielding isobutene and methoxy radicals as the major products.

Acknowledgment. The support of this work by the National Renewable Energy Laboratory (XAU-3-12228-02) is gratefully acknowledged. The constructive comments of the reviewers are appreciated.

References and Notes

(1) Finlayson-Pitts, B. J.; Pitts, Jr., J. N. *Atmospheric Chemistry*; Wiley: New York, 1986.
(2) Warnatz, J. In *Combustion Chemistry*; Gardiner, Jr., W. C., Ed.; Springer-Verlag: New York, 1984.
(3) *Chem. Eng. News* **1994** (Sept 26), 8−13.
(4) Chang, T. Y.; Hammerle, R. H.; Japar, S. M.; Salmeen, I. T. *Environ. Sci. Technol.* **1991**, *25*, 1190.
(5) Taylor, P. H.; Rubey, W. A.; Shanbhag, S.; Dellinger, B. NREL/TP-425-6650; National Renewable Energy Laboratory: Golden, CO, 1994.
(6) Whitney, K. NREL/TP-425-7528; National Renewable Energy Laboratory: Golden, CO, 1995.
(7) Gabele, P. *J. Air Waste Manage. Assoc.* **1995**, *45*, 770.
(8) "Guidance on Estimating Motor Vehicle Emission Reductions from the Use of Alternative Fuels and Fuel Blends. US-EPA, Report No. 1 EPA-AA-TSS-PA-87-4; Ann Arbor, MI, 1988.
(9) Taylor, P. H.; Shanbhag, S.; Rahman, M.; Dellinger, B. NREL/TP-425-7607; National Renewable Energy Laboratory: Golden, CO, 1995.
(10) Shanbhag, S.; Taylor, P. H.; Dellinger, B. The Origin and Fate of Organic Pollutants from the Combustion of Alternative Fuels. Proceedings of the 11th International Symposium on Alcohol Fuels, Sun City, South Africa, 1996.
(11) Taylor, P. H.; Cheng, L.; Dellinger, B. In Alternative Fuel: Composition, Performance, Engines, and Systems; SAE Technical Paper Series #961088, Warrendale, PA, 1996.
(12) Japar, S. M.; Wallington, T. J.; Richert, J. F. O.; Ball, J. C. *Int. J. Chem. Kinet.* **1990**, *22*, 1257.
(13) Tuazon, E. C.; Carter, W. P. L.; Aschmann, S. M.; Atkinson, R. *Int. J. Chem. Kinet.* **1991**, *23*, 1003.
(14) Taylor, P. H.; Jiang, Z.; Dellinger, B. *Int. J. Chem. Kinet.* **1993**, *25*, 9.
(15) Jiang, Z.; Taylor, P. H.; Dellinger, B. *J. Phys. Chem.* **1993**, *97*, 5050.

(16) Fang, T. D.; Taylor, P. H.; Dellinger, B. *J. Phys. Chem.* **1996**, *100*, 4048.
(17) Selwyb, G.; Podolske, J.; Johnstron, H. S. *Geophys. Res. Lett.* **1977**, *4*, 427.
(18) Simonaitis, R.; Heicklen, J. *J. Phys. Chem.* **1973**, *77*, 1932.
(19) Fang, T. D. Ph.D. Dissertation, University of Dayton, 1996.
(20) Calvert, J. G.; Pitts, Jr., J. N. *Photochemistry*, 2nd ed.; Wiley: New York, 1967.
(21) Perry, R. A.; Atkinson, R.; Pitts, Jr., J. N. *J. Chem. Phys.* **1977**, *67*, 611.
(22) Tully, F. P.; Droege, A. T. *Int. J. Chem. Kinet.* **1987**, *19*, 251.
(23) Wallington, T. J.; Liu, R.; Dagaut, P.; Kurylo, M. J. *Int. J. Chem. Kinet.* **1988**, *20*, 41.
(24) Wallington, T. J.; Andino, J. M.; Skewes, L. M.; Siegl, W. O.; Japar, S. M. *Int. J. Chem. Kinet.* **1989**, *21*, 993.
(25) Nelson, L.; Rattigan, O.; Neavyn, R.; Sidebottom, H.; Treacy, J.; Nielsen, O. J. *Int. J. Chem. Kinet.* **1990**, *22*, 1111.
(26) Mellouki, A.; Teton, S.; Le Bras, G. *Int. J. Chem. Kinet.* **1995**, *27*, 791.
(27) Atkinson, R. *J. Phys. Chem. Ref. Data* **1990**, *Monogr. 1*.
(28) Cox, R. A.; Goldstone, A. *Proceedings, Second European Symposium on the Physico-Chemical Behavior of Atmospheric Pollutants*; D. Riedel Publishing: Dordrecht, Holland, 1982; p 112.
(29) Bennett, P. J.; Kerr, J. A. *J. Atmos. Chem.* **1990**, *4*, 253.
(30) Smith, D. F.; Kleindienst, T. E.; Hudgens, E. E.; McIver, C. D.; Bufalini, J. J. *Int. J. Chem. Kinet.* **1991**, *23*, 907.
(31) Rubey, W. A.; Striebich, R. C.; Taylor, P. H. Unpublished results.